EVALUATION OF GOLD MINERALISATION POTENTIAL USING AIRBORNE MAGNETIC AND GEOELECTRICAL METHODS WITHIN NW NIGERIA

[1]A.I. AUGIE, [2]M.N. YAHAYA, [3]A. ADAMU

[1,3]Department of Applied Geophysics, Federal University Birnin Kebbi, Nigeria. ORCID ID: 0000-0001-8554 8531
[2]Department of Physics with Electronic, Federal University Birnin Kebbi, Nigeria
E-mail: [1]ai.augie@fubk.edu.ng

Abstract - This study delineated the potential zones for gold mineralisation using aeromagnetic, 2D electrical resistivity tomography (ERT), and induced polarisation (IP) techniques. Half-degree airborne magnetic data sheets of 96_Shanga and 119_Yelwa that covered the study area were obtained from the Nigerian Geological Survey Agency (NGSA). These data were processed and analysed using a novel total gradient amplitude coupled with centre for exploration targeting (TGA-CET) technique developed by Oasis Montaj Geosoft. The TGA-CET results revealed areas of high amplitude magnetic anomalies and major magnetic structures (lineaments). In comparison to the geological setting of the area, the region is associated with Granite Gneiss, Migmatite Augen Gneiss, Amphibole Schist, Amphibolite, Medium to Coarse-Grained Biotite, Granite Porphery. Major zones of structures and strong magnetic anomalies were found in the eastern regions of NE Shanga, Rigau, Fakai, Ngaski, and Magama, which are consistent with previous magnetic studies undertaken in the area. These areas could be favoured for metallic minerals, particularly gold mineralisation. However, the region of NE Shanga identified by the magnetic approach for potential gold mineralisation was further studied using 2D ERT and IP detailed techniques in a dipole-dipole array. The geoelectric technique results for profiles 1 and 2 identified three significant zones of gold mineralisation potential, marked as G1, G3, and G. These locations feature low/high resistivity (3.86 to 373 Ωm/2913 to 8099 Ωm) and high chargeability (≥ 20 msec), indicating potential for metallic mineral exploration, particularly gold. The zones are located in the southern part of the Sabon Gari area, Kebbi state. The results of integrated geophysical techniques produced a database of precise coordinates, lateral lengths, and thickness/depths for prospective gold mineralisation zones. This database could aid in the exploration of gold minerals in the region.

Keywords - Gold Mineralisation Zones, Improved Total Gradient Amplitude (TGA) associated with Centre for Exploration Targeting (TGA-CET), Electrical Resistivity Tomography (ERT) and Induce Polarisation (IP)

I. INTRODUCTION

Nigeria is rich in solid minerals, particularly gold, which is widely distributed throughout the country (Garba, 2000 and 2003; Olalekan et al., 2016). Gold deposits in Nigeria are usually visible in quartz veins, but they can also be found as inclusions within certain ore minerals in a variety of metasedimentary and meta-igneous rocks across the supracrustal rocks of the schist belts (Ramadan and AbduelFattah, 2010; Sani et al., 2019).

The research region is in southern Kebbi state, between latitudes 10°30′0″N and 11°30′0″N, and longitudes 4°30′0″E and 5°0′0″E. The following local government areas (LGAs) comprise up the area: Fakai, Koko Besse, Shanga, Yauri, Ngaski, Agwara, Borgu, and Magama. Geologically, the area is located in foundation complex rocks as well as some sedimentary basin sections.

It is primarily supported by Pan-African Older Granitoid and some areas of the Gwandu Formation, Nufe Formation, Mangrove Swamps, and Per-Alaklin Younger Granitoids (NGSA, 2006).
These consists of; Rhyolite, biotite-granite, granite, meta-conglomerate, quartz-mica schist, migmatite Augen Gneiss, gneiss, sandstones, ironstones, and laterites.

The research's review of previous geophysical studies conducted in the area by; Ramadan and Abdel Fattah (2010), Bonde et al. (2019), Lawali et al. (2020), Augie et al. (2022), Augie et al. (2024) and Salako, et al. (2024), revealed that the estimated mineralisation potential is solely based on aeromagnetic and aero-radiometric data. The results reveal that the major structural trends were along the ENE-WSW, NE-SW, and E-W directions, with minor trends along the NW-SE, NNE-SSW, NNW-SSE, and N-S. These results are in line with the overall regional structural trend, which is a dip to the northwest. It is also revealed that the basement complex, which may contain valuable minerals, dominates the northern and southern parts of the area.
However, earlier geophysical studies in the area have failed to apply improved edge detection approaches such as Total Gradient Amplitude coupled with centre for exploration targeting (TGA-CET) for better lineament detection. The research region is located in a low-latitude zone; some previous geophysical studies did not employ a reduction-to-equator (RTE) filter to centralise the anomalies. According to Holden et al. (2008) and Core et al. (2009), to avoid anomalous noise in north-south signal results, a separate amplitude must be corrected at low latitudes, as in RTE-filtered data. Similarly, previous study relied solely on secondary data, and the abnormal zones revealed during aeromagnetic experiments

were not further investigated. Furthermore, a database consisting of precise location, length, and depth for gold mineralisation potential and its associated mineralisation has not been produced in the area.

This study used improved integrated geophysical techniques such as Total Gradient Amplitude associated with centre for exploration targeting (TGA-CET), 2D ERT, and IP to locate probable gold-bearing alteration zones and further subsurface striations that could host other mineralisation. The search began with a reconnaissance survey utilising the TGA-CET approach to identify structures capable of containing the minerals in relation to the exploration goal. The results of integrated geophysical techniques were used to build a conceptual model of gold mineralisation potential in the studied area.

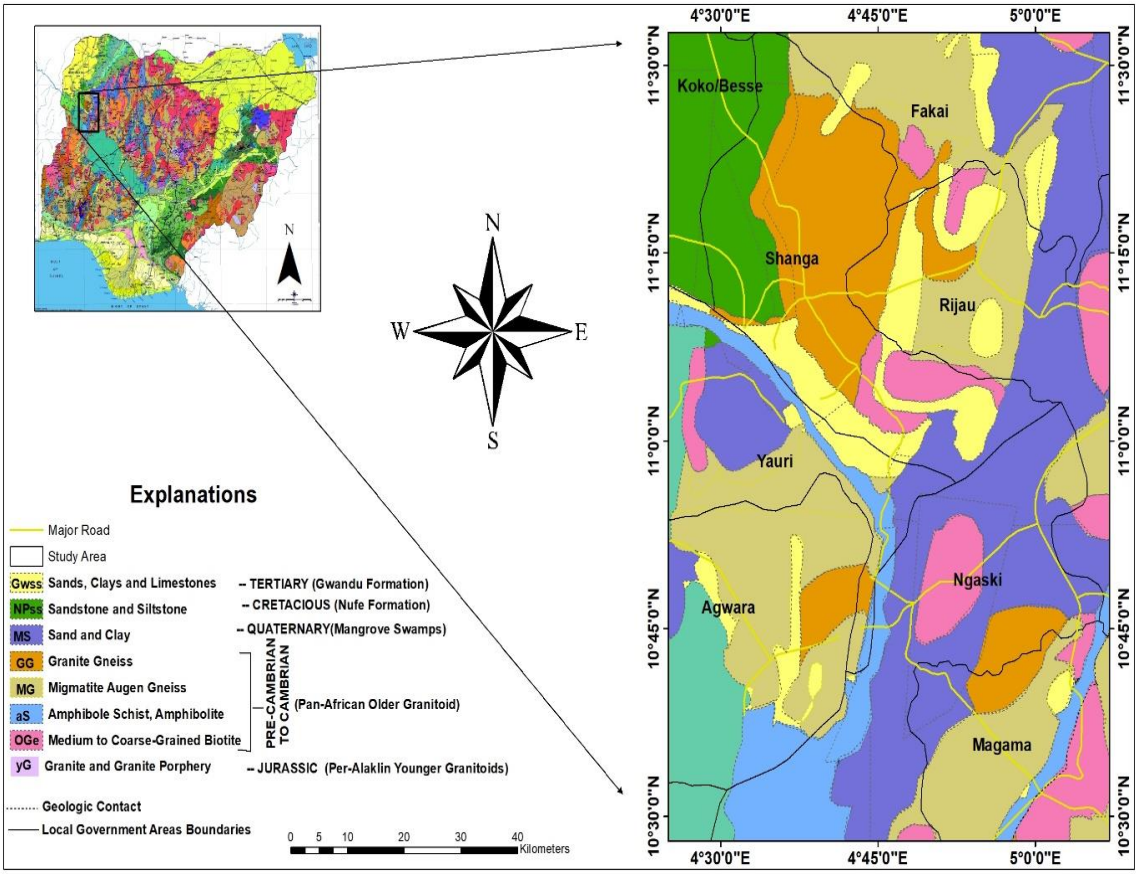


Figure 1: Location and geological setting of the study area (NGSA, 2016)

II. METHODS

2.1 Aeromagnetic Method

Fugro airborne surveys conducted aeromagnetic surveys over portions of the country for the Federal Government of Nigeria in 2010, and the data is managed by the Nigeria Geological Survey Agency (NGSA).

This work used two (2) aeromagnetic datasets from the study area. The datasets are known as Shanga-96 and Yelwa-118. The data was acquired using the high-resolution survey settings depicted in Figure 2. The magnetic dataset is collected by attaching a 3x3 Scintrex CS3 caesium vapour magnetometer sensor to the aircraft's fixed wing.

The data was corrected by subtracting the geomagnetic gradient (International Geomagnetic Reference Field, IGRF) from the main/core field. The magnetic anomaly (TMI anomaly) was derived by subtracting the generated core fields (DGRF for the epoch period) from the grid values.

The TMI anomaly map was further reduced to the magnetic equator to indicate an anomaly of the magnetised body that normally depends on the inclination, declination, local earth's field, and orientation of the body with respect to magnetic north. RTE and TGA-CET were used to further process, improve, and interpret the grid data (Figure 2).

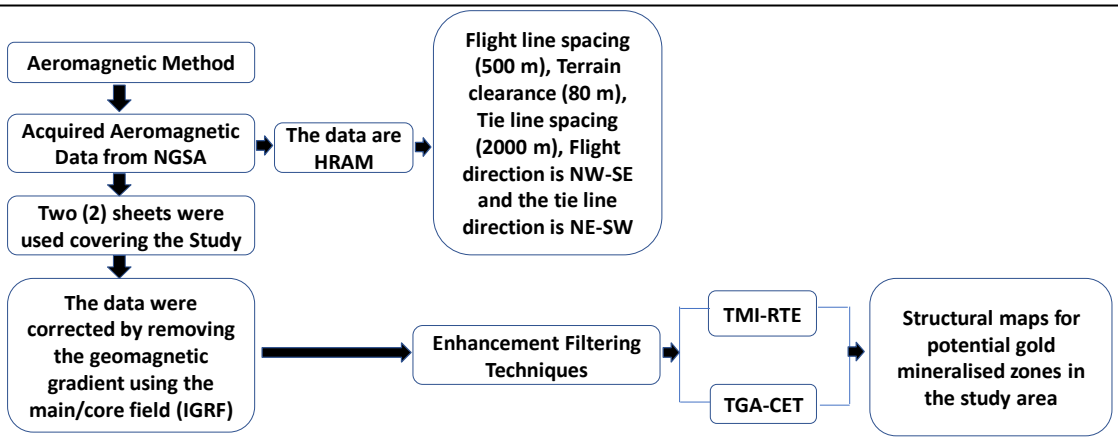


Figure 2: Workflow chart for aeromagnetic method.

2.2 Geoelectric Method

A detailed geophysical survey was carried out at the Shanga (Sabon Gari) of Kebbi state, NW Nigeria. These regions are some of the anomaly zones found by the aeromagnetic studies. A dipole-dipole arrangement with a minimum electrode separation (a) of 10.00 m was utilised to investigate fields over a 700 m2 area. Two (2) profiles were carried out for each 300 meters along the profile, orientated NW-SE. Measurements were taken at a 10 m electrode spacing with n ranging from 1 to 8 (Figure 3). The greater the increase in n, which also increases the electrode separation, the deeper the injected current travels. For the initial measurement, electrodes 1, 2, 3, and 4 were employed. Electrode 1 was employed as the second current electrode (C2) at 0 m, electrode 2 as the first current electrode (C1) at 10 m, electrode 3 as the first potential electrode (P1) at 20 m, and electrode 4 as the second potential electrode (C2) at 30m. These procedures were repeated along the profile line at intervals of 1a, 2a, 3a, 4a, 5a, 6a, 7a, and 8a between C1 and P1, with a = 10 m. At each measurement, the ground apparent resistivity and IP measurements were obtained. The obtained data were processed using the RES2DINV algorithm developed by Loke (1999), which automatically produces a 2D resistivity and IP model.

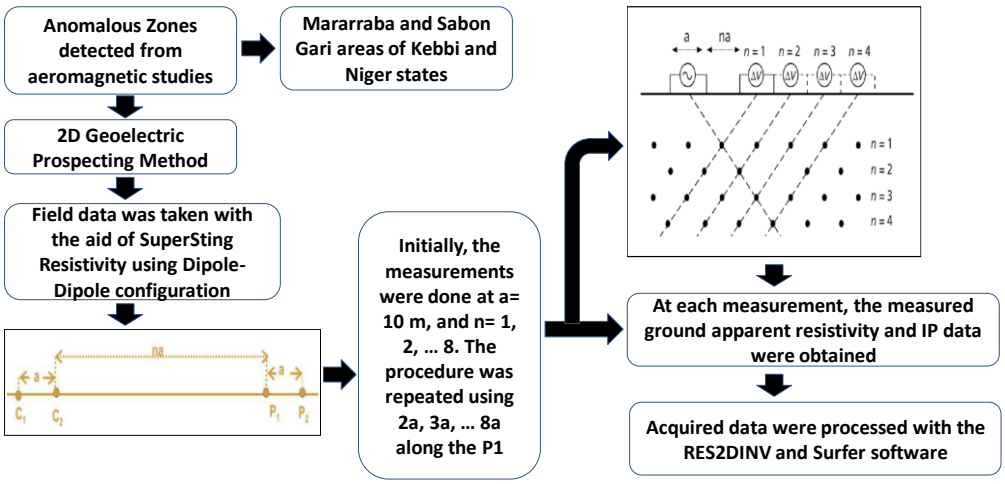


Figure 3: Workflow chart for geoelectric methods

III. RESULTS

3.1 Results from Airborne Magnetic Method

3.1.1 Total magnetic intensity and reduction to magnetic equator (TMI-RTE) result

Figure 4(a) is a coloured representation of the research area's reduced to the magnetic equator (RTE) map. This was achieved by subtracting the produced core fields (DGRF for the epoch period) from the TMI anomaly and reducing it to the magnetic equator (RTE). The high magnetic anomaly, ranging from -580.77 nT to -449.97 nT, are found in the southern section of the research area. Low magnetic anomalies ranging from -731.44 to -583.36 nT exist in the northern part of the study area (Figure 4a).

High negative values indicate high magnetic susceptibility zones because the magnetic equator is a zero-inclination zone and all rocks are polarised by the horizontal component of the Earth's magnetic field, which normally resists rock magnetisation. When the crustal field and other temporal effects are removed from the measured field, the resulting anomaly is usually negative over magnetic materials.

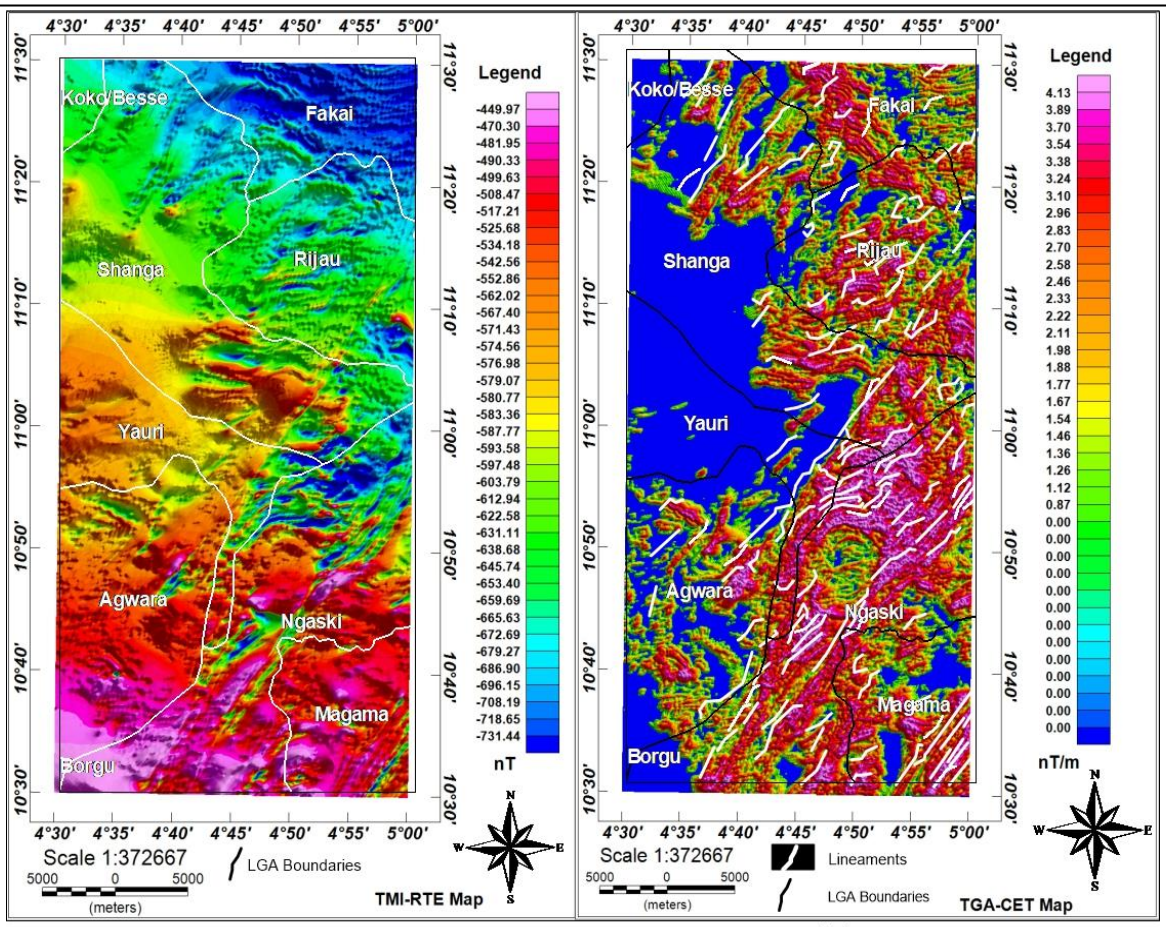


Figure 4: (a) Total magnetic intensity, which is reduced to magnetic equator (TMI_RTE) map (b) Total gradient amplitude coupled with center for exploration targeting (TGA-CET) map of the study area.

3.1.2 Total gradient amplitude (TGA) coupled with CET result

The TGA, when merged with the CET map (Figure 4b), enhanced the visibility of the variance in magnetisation of the magnetic sources across the field and also revealed the limits of abnormal texture. This filter improves the near-surface basement and structural features. Figure 4(b) shows that high magnetic anomalies combined with the zones of major lineament are associated with the existence of metallic minerals, as evidenced by the geological setting of the region. The low magnetic trend in blue/green colour ranges from 0.00 to 1.77 nT/m, while the high magnetic anomaly in red/pink colour range from 1.88 to 4.13 nT/m.

Low magnetic anomalies with low amplitude were delineated at Koko/Besse, the western part of Shagari, Yauri, Agwara, and Borgu. When contrasted to the area's geological setting, these zones were associated with sands, sandstones, siltstones, clays, and limestones. Hydrocarbon and energy minerals have the potential to have a significant impact on the Earth's materials.

The high magnetic/amplitude features anomalies associated with lineament are related with Granite Gneiss, Migmatite Augen Gneiss, Amphibole Schist, Amphibolite, Medium to Coarse-Grained Biotite, Granite Porphery (Figure 1). These regions are located in NE Shanga, Rigau, Fakai, Ngaski and Magama. When these zoens are compared to the susceptibility of common rocks and geological settings, it is obvious that the locations have a significant influence on high metallic minerals such as gold mineralisation.

3.2 Results from Geoelectric Methods

3.2.1 Resistivity and IP model for profile one (P1)

Figure 6(a) depicts the 2D resistivity model section along profile one (P1), which was subsequently transformed into a geologic section, as illustrated in Figure 6(b). It is oriented NW-SE and has a lateral extent of 300 meters. The profile lies between latitudes 11°5′24″N to 11°5′34.8″N and longitudes 4°43′8.4″E to 4°43′19.2″E (see Figure 5).

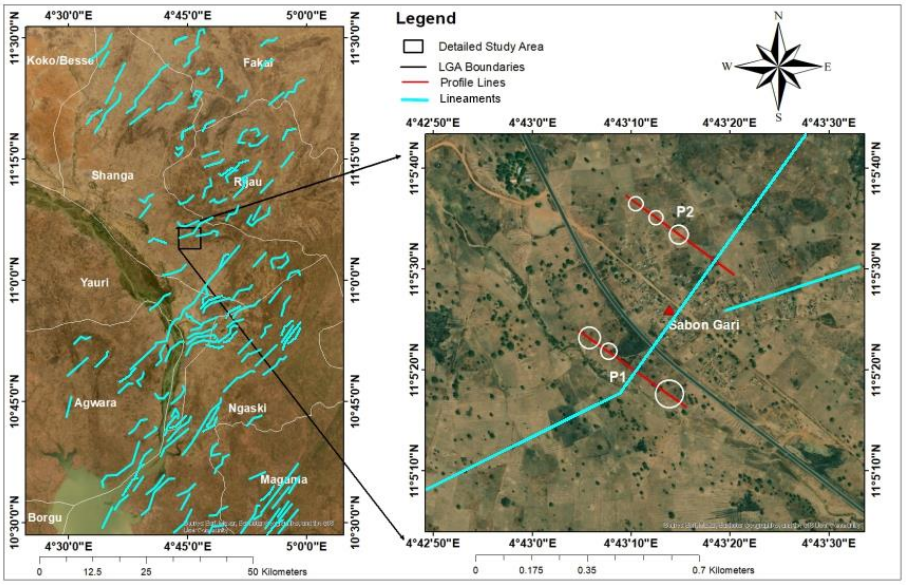


Figure 5: Field survey layout using the dipole-dipole electrode configuration and potential gold mineralisation zones of the study area

Lithology	Depth(m)	Thickness(m)	Resistivity range (Ωm)
Lateritic Sand	0-2	2	60-1000
Highly Decomposed Schist	2-10	8	10-500
Partially Decomposed Granite	10-15	12	100-1000
Quartzite's and Gneiss	15-21	16	200-100000

Table 1: A borehole/lithology log of southern part of Kebbi areas (SARDA, 1988; Osazuwa and Chii, 2010)

The subsurface feature of P1 was divided into four zones: G1, G2, G3, and G4. In comparison to Figure 6(a), the suggested subsurface lithology for highlights G1, G2, G3, and G4 from Table 1 could consist of lateritic soil, extensively decomposed schist, partially decomposed granite and quartzite, or quartzite/gneiss.

Zone G1 is associated with oxidised granite/quartzite and gneiss, and it could be related potential minerals, particularly gold. Zone G3 is also include metallic minerals since it developed dyke structures associated with partially decomposed granite and quartzite. These structures could have a significant impact on mineralisation, especially gold mineralisation. Figure 6(c) shows a two-dimensional chargeability section along P1. Zone G refers to areas with high chargeability (≥ 20 msec), which could be caused by metallic materials. These regions could be considered some of the most prospective for gold mineralisation exploration. The summary of the results was given in Table 2.

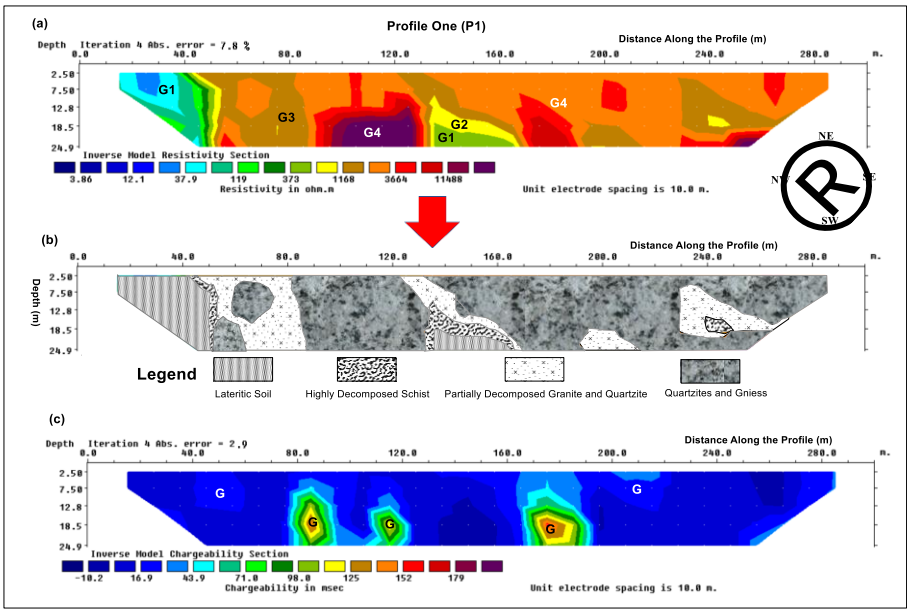


Figure 6: (a) Inverse model resistivity section (b) geologic section and (c) IP section for the dataset along profile one (P1)

3.2.2 Resistivity and IP model for profile two (P2)

Figure 7(a) depicts the 2D resistivity model section along profile two (P2), which was then translated into a geologic section, as illustrated in Figure 7(b). It is oriented NW-SE and has a lateral extent of 300 meters. The profile spans latitudes 11° 5' 37.32"N to 11° 5' 29.76"N, and longitudes 4° 43' 9.48"E to 4° 43' 20.28"E (Figure 5). The subsurface feature of P1 was divided into four zones: G1, G2, G3, and G4. In comparison to Figure 7(a), the suggested subsurface lithology for highlights G1, G2, G3, and G4 from Table 1 could include lateritic soil, highly decomposed schist, partially decomposed granite and quartzite, or quartzite/gneiss.

Zone G1 is associated with oxidised granite/quartzite and gneiss, and it may be connected to certain minerals, particularly gold. Zone G3 is also likely to include metallic minerals, as it generated the dyke structures associated with partially decomposed granite and quartzite. These structures may play an important role in defining minerals, particularly gold mineralisation. Figure 6(c) depicts the 2D chargeability section along P2, with high chargeability (≥ 20 msec) designated as zone G. These zones could form as a result of the presence of metallic minerals. These areas could be regarded some of the most likely regions to look for gold mineralisation. Table 2 presents a brief summary of the results.

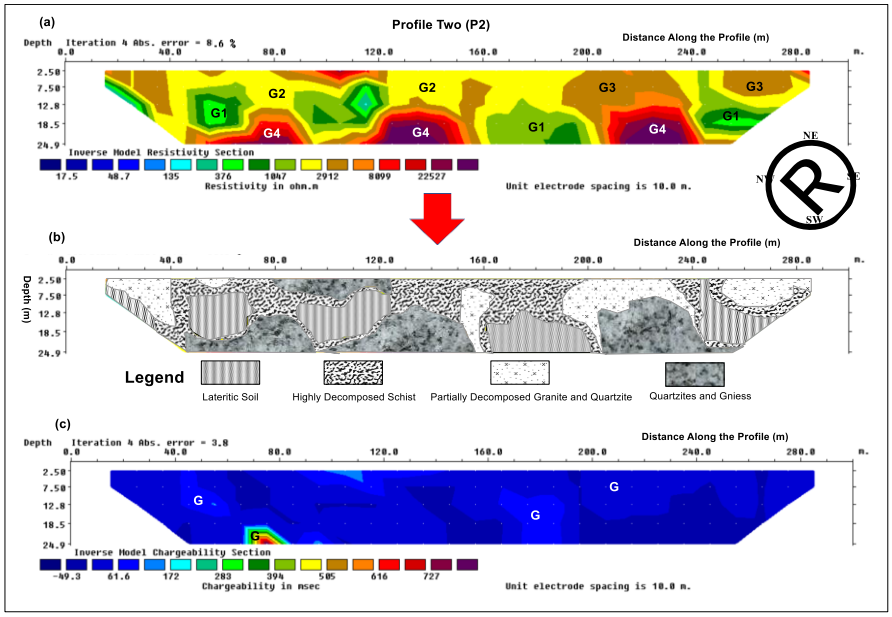


Figure 7: (a) Inverse model resistivity section (b) geologic section and (c) IP section for the dataset along profile two (P2)

Profile	Resistivity results				Induced polarisation (IP) results				Possible gold mineralisation potential remarks
	Zone	Resistivity ranges (Ωm)	Lateral lengths (m)	Depth/ Thickness (m)	Zone	Chargeability ranges (msec)	Lateral lengths (m)	Depth/ Thickness (m)	
P6	G1	3.86 to 373	5-45 and 130-165	24.9 and 18.5-24.9	A1	≥ 20	40-60, 75.5-120, 155-180 and 200-220	12.8, 24.9, 24.9 and 12.8	Yes
	G2	374 to 1168	40-45, 130-165 and 240-250	24.9, 7.5-18.5 and 12.8-18.5	-	-	-	-	No
	G3	41169 to 3664	50-80, 120-150, 190-210 and 230-270	24.9, 12.8, 18.5-24.9 and 2.5-18.5	-	-	-	-	Yes
	G4	3665 to 11488	50-60, 61-72, 80-130 and 132-290	12.8-24.9, 2.5-12.8, 24.9, 24.9	-	-	-	-	No
P7	G1	17.5 to 376	10-30, 45-70, 90-120, 160-200 and 250-270	2.5-18.5, 7.5-18.5, 7.5-18.5, 12.8-24.9 and 7.5-18.5	A1	≥ 61	1-60, 62-80, 70-130, 150-190, 192-260 and 265-300	24.9, 18.5-24.9, 24.9, 24.9, 18.5 and 18.5	Yes
	G2	377 to 2912	50-90 and 60-105	12.8, 18.5 and 12.8	-	-	-	-	No
	G3	2913 to 8099	10-40, 150-160, 190-235 and 250-290	12.8, 2.5, 12.8 and 7.5	-	-	-	-	Yes
	G4	8100 to 22527	45-90, 80-125, 00-150, and 200-240	12.8-24.9, 7.5, 12.8-24.9, 12.8-24.9	-	-	-	-	No

Table 2: Summary of results obtained from the integrated methods

IV. CONCLUSIONS

The use of improved TGA-CET techniques in this study revealed areas of high amplitude magnetic anomalies coupled with major magnetic structures (lineaments) associated with Granite Gneiss, Migmatite Augen Gneiss, Amphibole Schist, Amphibolite, Medium to Coarse-Grained Biotite, and Granite Porphery in comparison to the geological setting of the area. Major zones of structures and high magnetic/amplitude anomalies have been found in NE Shanga, Rigau, Fakai, Ngaski, and Magama, which are consistent with previous magnetic studies conducted in the region by Augie et al. (2024) and Salako et al. (2024). These areas could be favourable for metallic minerals, particularly gold mineralisation. However, among the aforementioned locations with probable gold mineralisation, NE Shanga was investigated further using 2D ERT and IP detailed techniques in a dipole-dipole configuration. The results along profiles 1 and 2 revealed three significant zones of gold mineralisation potential: G1 with resistivity values ranging from 3.86 to 373 Ωm, G3 with resistivity values ranging from 2913 to 8099 Ωm, and G with chargeability values > 20 msec. These zones could be considered as prospecting zones for metallic minerals, particularly for gold. The zones are located in the southern part of Sabon Gari, Kebbi State. The results of integrated geophysical techniques produced a database of accurate coordinates, lateral lengths, and thickness/depths for prospective gold mineralisation zones. This database could help with the exploration of gold minerals in the region.

ACKNOWLEDGEMENTS

The authors would like to express their profound appreciation to the Tertiary Education Trust Fund (TETFund) for funding this research.

REFERENCES

[1] Garba, I. (2000). Origin of Pan-African mesothermal gold mineralisation at Bin Yauri, Nigeria. Journal of African Earth Sciences, 31, 433–449

[2] Garba, I. (2003). Geochemical characteristics of mesothermal gold mineralisation in the Pan-African (600±150 Ma) basement of Nigeria. Applied Earth Science (Transaction of the Institution of Mining and Metallurgy, Section B), 112, 319–325

[3] Ramadan, T.M. & AbdelFattah, M.F., (2010). Characterization of gold mineralization in Garin Hawal area, Kebbi State, NW Nigeria, using remote sensing. Egyptian Journal of Remote Sensing and Space Science, 13(2), 153–163. https://doi.org/10.1016/j.ejrs.2009.08.001

[4] Sani, A.A., Augie, A.I. & Aku, M.O. (2019). Analysis of gold mineral potentials in Anka schist belt north western Nigeria using aeromagnetic data interpretation, Journal of the Nigerian Association of Mathematical Physics, 52, 291-298

[5] NGSA, (2006). Nigerian Geological Survey Agency, Nigeria.

[6] Augie, A. I., Salako, K. A., Bery, A. A., Rafiu, A. A., & Jimoh, M. O. (2024). Integrated geophysical investigation using aero-radiometric and electrical methods for potential gold mineralization within Yauri/ Zuru schist belts, Kebbi State NW Nigeria. Earth Sciences Research Journal, 28(2), 137-146. https://doi.org/10.15446/esrj.v28n2.112066

[7] Augie, A.I., Salako, K.A., Rafiu, A.A. & Jimoh, M.O. (2022). Geophysical assessment for gold mineralisation potential over the southern part of Kebbi State using aeromagnetic data. Geology, Geophysics & Environment, 48 (2), 177–193. https://doi.org/10.7494/geol.2022.48.2.177.

[8] Salako, K.A., Adetona, A.A., Rafiu, A.A., Augie, A.I., Jimoh, M.O., Alkali, A., Muriana, R.A., Lawrence, J.O. Integrated geophysical Investigation for gold mineralization potential over southern parts of Kebbi state and its Environs, northwestern Nigeria. Heliyon 10 (2024) e34093. https://doi.org/10.1016/j.heliyon.2024.e34093

[9] Core, D., Buckingham, A. & Belfield, S. (2009). Detailed structural analysis of magnetic data-done quickly and objectively. SGEG Newsletter, 1(2), 15–21.

[10] Holden, E.J., Dentith, M. & Kavesi, P. (2008). Towards the automatic analysis of regional aeromagnetic data to identify regions prospective for gold deposits. Computer Geoscience, 34, 1505–1513, https://doi.org/10.1016/j.cageo. 2007.08.007

[11] Lawali, S., Salako, K.A. & Bonde, D.S. (2020). Delineation of mineral potential zones over lower part of Sokoto Basin, northwestern Nigeria using aeromagnetic data. Academic Research International, 11(2), 19–29

[12] Loke, H.M. (1999). Electrical imaging surveys for environment and engineering studies (practical guide to 2D and 3D survey). Earth Sciences, 44(1), 131–152.

[13] Olalekan, O., Afees, O. & Ayodele, S. (2016). An empirical analysis of the contribution of mining sector to economic development in Nigeria. Khazar Journal of Humanities and Social Sciences, 19(1), 88–106.

[14] .Osazuwa, I. B. and Chii, E.C. (2010). Two-dimensional electrical resistivity survey around the periphery of an artificial lake in the precambrian basement complex of northern Nigeria. International Journal of Physical Science, 5(3): 238–245.

[15] SARDA, (1988) Sokoto agricultural and rural development authority: Sokoto Fadama.

★★★